Hindawi Publishing Corporation
International Journal of Distributed Sensor Networks
Volume 2012, Article ID 940302, 11 pages
doi:10.1155/2012/940302

Research Article

Investigation of Uncoordinated Coexisting IEEE 802.15.4 Networks with Sleep Mode for Machine-to-Machine Communications

Chao Ma,[1] Jianhua He,[1] Zuoyin Tang,[1] Wenyang Guan,[2] and Yue Li[2]

[1] *School of Engineering and Applied Science, Aston University, Birmingham B47ET, UK*
[2] *College of Engineering, Swansea University, Wales SA28PP, UK*

Correspondence should be addressed to Wenyang Guan, 440501@swansea.ac.uk

Received 20 April 2012; Revised 15 June 2012; Accepted 25 June 2012

Academic Editor: Lin Bai

The low-energy consumption of IEEE 802.15.4 networks makes it a strong candidate for machine-to-machine (M2M) communications. As multiple M2M applications with 802.15.4 networks may be deployed closely and independently in residential or enterprise areas, supporting reliable and timely M2M communications can be a big challenge especially when potential hidden terminals appear. In this paper, we investigate two scenarios of 802.15.4 network-based M2M communication. An analytic model is proposed to understand the performance of uncoordinated coexisting 802.15.4 networks. Sleep mode operations of the networks are taken into account. Simulations verified the analytic model. It is observed that reducing sleep time and overlap ratio can increase the performance of M2M communications. When the networks are uncoordinated, reducing the overlap ratio can effectively improve the network performance.

1. Introduction

The increasingly popular M2M technology can enable machines to communicate directly with one another through wireless and/or wired system [1, 2]. With the increasing volume of wireless networks in recent years, the information can be exchanged between machine devices much easier and faster at low cost, which makes M2M technology more attractive to business as well as customers due to its huge potential on cost reduction and services improvement [3, 4]. Effective and reliable support from wireless networks for communications between the number of M2M devices is pivotal to the success of M2M technology. This paper aims to study the effectiveness of IEEE 802.15.4 network technology on support of M2M communications [5]. With increasing number of M2M devices which may be connected by IEEE 802.15.4 network, it is very likely to witness that multiple 802.15.4 networks are closely and independently deployed for M2M appellations. The interference of each other and hidden terminal problem may arise among these M2M devices, which can become severe problems for 802.15.4 networks-based M2M applications.

In this paper we investigate the issues of multiple uncoordinated coexisting 802.15.4 networks when they are closely deployed with sleep mode. Two representative network scenarios where two 802.15.4 networks are working in the sleep mode with different overlap ratios in the channel access periods are presented. We propose an analytic model to predict the system throughput and energy consumption with different media access control (MAC) parameters, frame length, the number of network devices for each network, and overlap ratios. The results show that the impact of uncoordinated multiple networks operations can lead to significant system performance drop when their channel access periods are most overlapped. The approaches of reducing sleep time and overlap ratio to increase the system performance are also studied. The analytic model is verified by simulations.

In the literatures, simulation-based evaluation of single 802.15.4 network has been widely reported including [6, 7]. Additionally, many analytic models have been proposed to capture the throughput and energy consumption performance of single 802.15.4 network with either saturated or

unsaturated traffic. The limited scalability of the 802.15.4 MAC was pointed out by Yedavalli and Krishnamachari [8] where the performance in terms of throughput and energy consumption are studied. They showed that 802.15.4 MAC performed poorly when the number of contending devices was high. Mišić et al. proposed a Markov model to evaluate the throughput of 802.15.4 networks with unsaturated downlink and uplink traffic [9]. However, their analytical models do not have high accuracy. A simplified Markov model was proposed in [10], in which a geometric distribution was used to approximate the uniform distribution for the random backoff counter. But the approximation results in large inaccuracy in throughput prediction. A three-dimensional Markov model was proposed in [11] to evaluate the throughput of slotted carrier sense multiple access (CSMA). However, the state transitions in [11] were not correctly modelled. The model was revised with improved accuracy in [12]. Both Pollin et al. [13] and Singh et al. [14] also considered a star network topology and analysed the MAC protocol performance under assumption that saturated traffic conditions. They found out that a large fraction of packets was dropped during the channel access, and the dropping probability increases with the number of sensor devices. Park et al. [15] and He et al. [16] developed accurate analytical modes for 802.15.4 MAC protocol in the beacon-enabled mode for star network topology. In addition, the performance analysis was mainly targeted at validating the accuracy of the proposed model. Energy consumption and throughput performance of 802.15.4 MAC was analysed in [17]. However, none of these works has studied the uncoordinated operations of multiple coexisting 802.15.4 networks with sleep mode.

The remainder of this paper is organised as follows. In Section 2, we introduce the superframe structure and channel access algorithm of IEEE 802.15.4 standard briefly. Two scenarios and model assumption of the analytic model are introduced in Section 2 and the analytic model of two uncoordinated networks is presented in Section 3. Section 4 discusses the numerical results and performance analysis. The conclusions and future works are in Section 5.

2. Channel Access Algorithm of IEEE 802.15.4

An IEEE 802.15.4 network can work either in nonbeacon-enabled or in beacon-enabled mode [5]. In the nonbeacon-enabled mode, there are no regular beacons, and devices communicate with each other using unslotted CSMA-CA algorithm. In the beacon-enabled mode, the coordinator transmits regular beacons for synchronisation and association procedures to control communication. A superframe structure is imposed in the beacon-enabled mode as shown in Figure 1, whose format is defined by the coordinator. The superframe is bounded by network regular beacons, and can have an active portion and an optional inactive portion. All communications take place in the active period while devices are allowed to enter a low-power (sleep) mode during the inactive period. The structure of this superframe is described by the values of *macBeaconOrder* (*BO*) and *macSuperframeOrder* (*SO*). The BO describes the beacon interval (BI), the SO describes the length of superframe duration (SD), and they are related, respectively, as follow:

$$\begin{aligned} \mathrm{BI} &= \mathrm{aBaseSuperframeDuration} \times 2^{\mathrm{BO}}, \\ \mathrm{SD} &= \mathrm{aBaseSuperframeDuration} \times 2^{\mathrm{SO}}, \end{aligned} \tag{1}$$

where aBaseSuperframeDuration = 960 symbols and $0 \leq \mathrm{SO} \leq \mathrm{BO} \leq 14$.

The active portion of each superframe shall be composed of two parts: a contention access period (CAP) and an optional contention-free period (CFP). The CAP shall start immediately following the beacon and complete before the beginning of CFP on a superframe slot boundary. If the CFP is zero length, the CAP shall complete at the end of the active portion of the superframe. We neglect every CFP in this study, because it is designed for low-latency applications requiring specific data bandwidth which means only CAP in each active portion of superframe structure. In CAP, communication among devices uses slotted CSMA-CA algorithm for contention access. The 802.15.4 slotted CSMA-CA algorithm operates in unit of backoff slot. One backoff slot has the length of 20 symbols. In the rest of the paper backoff slot is simply called slot unless otherwise specified.

According to the acknowledgement (ACK) of successful reception of a data frame, the slotted CSMA-CA algorithm can be operated in two modes: ACK mode, if an ACK frame is to be sent and non-ACK mode, if an ACK frame is not expected to be sent. In this paper we will work on the non-ACK mode. In the non-ACK mode, every device in the network maintains three variables for each transmission attempt: NB, W, and CW. NB denotes the backoff stage, representing the backoff times that have been retried in the slotted CSMA-CA process while one device is trying to transmit a data frame in each transmission. W denotes the backoff window, representing the number of slots that one device needs to back off before clear channel assessment (CCA). CW represents the contention window length and is used to determine how many slots for the CCA before transmissions. CW will be set to two before each transmission and reset to two when the channel is sensed busy in CCAs.

Before each device starts a new transmission attempt, NB sets to zero and W sets to W_0. The backoff counter chooses a random number from $[0, W_0 - 1]$ and it decreases every slot without sensing channel until it reaches zero. If the number of backoff slots is greater than the remaining number of slots in the CAP, the MAC sublayer shall pause the backoff countdown at the end of the CAP and resume it at the start of the CAP in the next superframe [5]. If the number of backoff slots is less than or equal to the remaining number of slots in the CAP, the MAC sublayer shall check whether the number of remaining slots in current CAP is enough to complete the two CCAs and the frame transmission when backoff counter reaches zero. If the two CCAs and the frame transmission can be completed, the MAC sublayer shall request that the PHY perform the first CCA (denoted by CCA1) when backoff counter reaches zero. If channel is idle at CCA1, CW decreases one and the second CCA (denoted

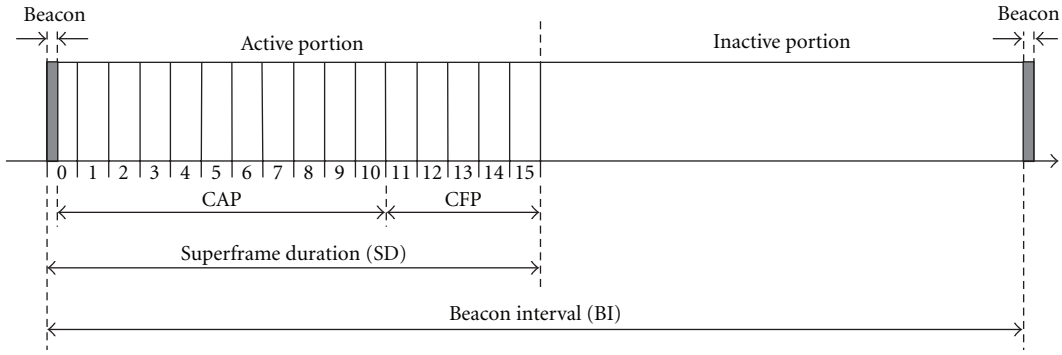

Figure 1: An example of the superframe structure. In this case, the beacon interval, BI, is twice as long as the active superframe duration, SD, and it contains CFP.

by CCA2) will be performed after CCA1. If channel is idle for both CCA1 and CCA2, the frame will be transmitted in next slots. If channel is busy in either CCA1 or CCA2, CW resets to two, NB increases by one, and W is doubled but not exceed W_x. If NB is smaller or equal to the allowed number of backoff retries macMaxCSMABackoffs (denoted by m), the above backoff and CCA processes are repeated. If NB exceeds m, the CSMA-CA algorithm ends. If two CCAs and the frame transmission cannot be completed in the remaining CAP, the MAC sublayer shall wait until the start of the CAP in the next superframe and apply a further random backoff delay before evaluating whether it can proceed again.

3. Model Assumption

There can be many scenarios with which the 802.15.4 networks may or may not interfere with each other if their operations are not coordinated when multiple 802.15.4 networks are deployed independently and closely. We assume two 802.15.4 networks are deployed closely and two simple representative scenarios are considered to focus on obtaining insights to the impact of uncoordinated operations on system performance.

We consider a star network topology with a PAN coordinator. These two networks are labelled by NET1 and NET2 with N_1 and N_2 denoting the number of basic devices in addition to one coordinator in each network, respectively. All the devices in its own network are within communication ranges of each other. Only uplink traffic from the basic devices to the coordinator in each network is considered. Each data frame has a fixed length which requires L slots to transmit over the channel. The data payload in MAC layer frame is fixed L_d slots, which is transmitted as the MAC payload in the MAC protocol data unit. In our scenarios, we assume that the two networks are both transmitting equal length of data payload L_d slots using the same L slots through the channel. We assume a saturated traffic with non-ACK mode, which means that each device has always traffic to send frames to its coordinator. The BOs of NET1 and NET2 are the same, which means the length of BIs of two networks are equal. The SOs of NET1 and NET2 are also set the same, which gives them equal active portions as well. We also consider an idle superframe structure, which means the active portions only consist of CAP without CFP, and an idle channel over which a frame fails if and only if collision happens.

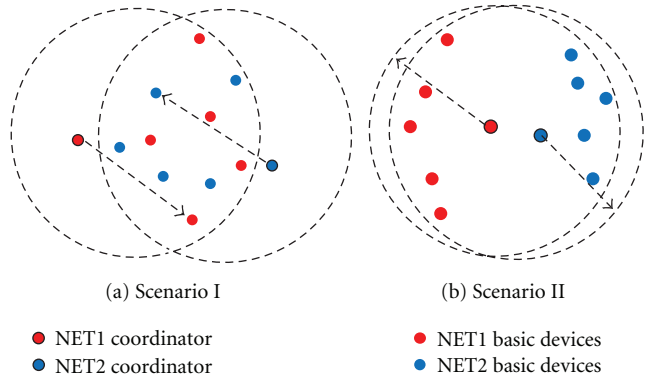

Figure 2: Communication range of each network is fully overlapped; (a) basic devices from two networks can detect each other's transmissions through CCAs; (b) basic devices from each network cannot detect transmission from other network's transmission through CCAs.

(1) Scenario I. For this scenario we assume that both considered networks are operated on the same frequency channel and the communication range of each network is fully overlapped as shown in Figure 2(a). We consider the beacon-enabled mode as mentioned in the previous section. Each network has a coordinator, which is responsible for broadcasting the beacon frames in the beginning of superframes. For simplicity, we assume that the beacons from any network can be correctly received by all the basic devices which belong to that network. The two networks share the whole channel frequencies, which means they can detect each other's transmissions through CCAs. For this scenario, the CAPs from each network can be partially overlapped or fully overlapped with different overlap ratio g as shown in Figure 3. When $g = 1$, which is the worst case that the two networks are fully overlapped in channel access periods, and when $g = 0$, which means there is no interference between these two networks.

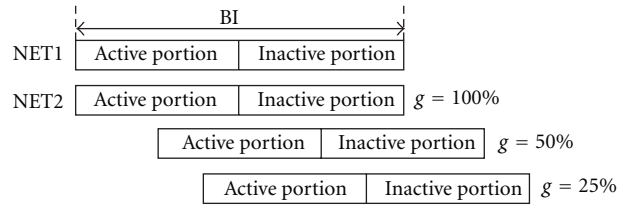

Figure 3: Illustration of channel access periods overlap in the superframe structure with different overlap ratio g, where g is the ratio of the number of slots in overlapped part to the number of slots in CAP, $0 \le g \le 1$.

(2) Scenario II. In this scenario, we assume these two networks share the channel frequencies and their communication range is fully overlapped as shown in Figure 2(b). We consider that the basic devices of each network can only hear transmissions from the other devices in its own network but cannot detect transmissions from other networks, which means that the CCA detections for each device are not affected by the channel activities from the other networks. This could happen because the distance between the basic devices and the two networks is too far to hear each other, although they operate on the same frequency channel. But the coordinators for the networks can detect transmissions from all the basic devices not only their own networks but also the other networks. With this assumption hidden terminals are present from neighbour networks. The transmissions could be collided by the data from other networks if they have overlap in the channel access portion. The same with Scenario I, when $g = 1$, which is the worst case that the CAPs of two networks are fully overlapped, and $g = 0$ means there is no interference in the CAPs for each network. We assume that the beacons from either network can be correctly received by all the devices belong to that network.

4. Analytic Model for Scenarios

4.1. Analytic Model of Scenario I. In the superframe structure, there is no activity from any device in the inactive portion for each network. The system performance of networks in CAP for Scenario I could be analysed separately with two parts according to different overlap ratio g: nonoverlapped and overlapped part.

For the nonoverlapped part, the performance of networks could be analysed with the existing analytic model for single 802.15.4 network proposed in [12]. According to the idea of performance modelling in [12], the nonoverlapped part channel states sensed by each device of either 802.15.4 network can be modelled by a renewal process, which starts with an idle period and followed by a fixed length of L slots (frame transmission), as shown in Figure 4.

The idle period depends on the random backoff slots and the transmission activities from each device. It is noted that the maximal number of idle slots is $W_x - 1$ plus two slot CCAs. On the other hand, the slotted CSMA-CA operations of each individual device could be modelled by a Markov chain with finite states. Let $p_{n,k}$ denote the probability of a transmission from devices in network n (n represents network identification, being 1 or 2) other than a tagged basic device in network n starting after exactly kth idle slots since the last transmission, where $k \in [0, W_x + 1]$ [12]. The transmission probability of a basic device in a general backoff slot can be calculated with the Markov chain constructed for each device.

Without loss of generality we consider NET1 and a tagged basic device in NET1. For the tagged basic device, its Markov chain consists of a number of finite states and each corresponds to a state of the CSMA-CA algorithm in one slot. These finite states are introduced below. Let $\overline{M}$ denote the steady-state probability of a general state M in the Markov state space. For simplicity we ignore the subscript "1" which corresponds to NET1 in the Markov states. In the following derivation we assume NET1 and NET2 use the same set of MAC parameters. It is trivial to extend to the cases with different sets of MAC parameters.

(1) Busy State. Denoted by $B_{i,j,l}$, during which at least one device other than the tagged basic device transmits the lth part of a frame of L slots, with the backoff stage and backoff counter of the tagged basic device being i and j, respectively, where $i \in [0, m]$, $j \in [0, W_i - 1]$, and $l \in [2, L]$, W_i is the minimum of $2^i W_0$ and W_m [12]:

$$\overline{B}_{0,j,2} = \sum_{k=2}^{W_0-1} p_k \overline{K}_{0,j+1,k} + \frac{1}{W_0} \sum_{k=2}^{W_m} p_k \left(\overline{K}_{m,0,k} + \overline{C}_{m,k}\right), \quad i = 0,\ j \in [0, W_0 - 1],$$

$$\overline{B}_{i,j,2} = \sum_{k=2}^{W_i-1} p_k \overline{K}_{i,j+1,k} + \frac{1}{W_i} \sum_{k=2}^{W_i-1} p_k \left(\overline{K}_{i-1,0,k} + \overline{C}_{i-1,k}\right), \quad i \in [1, m],\ j \in [0, W_i - 1],$$

$$\overline{B}_{i,j,l} = \begin{cases} \overline{B}_{0,j+1,l-1} + \dfrac{\overline{B}_{m,0,l-1}}{W_0}, & i = 0,\ j \in [0, W_i - 1], \\ \overline{B}_{i,j+1,l-1} + \dfrac{\overline{B}_{i-1,0,l-1}}{W_i}, & i \in [1, m],\ j \in [0, W_i - 1]. \end{cases} \tag{2}$$

(2) Backoff State. Denoted by $K_{i,j,k}$, during which the tagged basic device backoff with backoff counter being j at backoff stage i, after k idle slots since the last transmission, where $i \in [0, m]$, $j \in [0, W_i - 1]$, and $k \in [0, W_i - 1]$ [12]:

$$\overline{K}_{0,j,0} = \overline{B}_{0,j+1,L} + \frac{\left(\overline{B}_{m,0,L} + \overline{T}_L\right)}{W_0}, \quad i = 0,\ j \in [0, W_0 - 1],$$

$$\overline{K}_{i,j,0} = \overline{B}_{i,j+1,L} + \frac{\overline{B}_{i-1,0,L}}{W_i}, \quad i \in [1, m],\ j \in [0, W_i - 1],$$

$$\overline{K}_{i,j,k} = \begin{cases} \overline{K}_{i,j+1,k-1}, & k \in [1, 2], \\ (1 - p_{k-1}) \overline{K}_{i,j+1,k-1}, & 3 \le k \le W_i - 1. \end{cases} \tag{3}$$

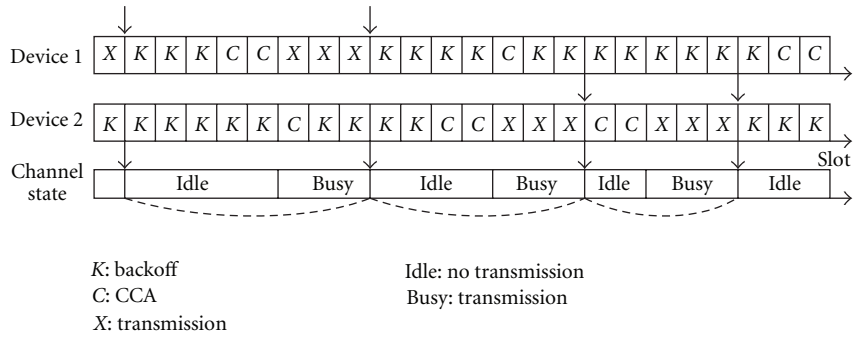

Figure 4: Example of channel renewal process for 802.15.4 networks. A random number of idle slots followed by a fixed length of transmission in the CAP.

(3) Sensing State. Denoted by $C_{i,k}$, during which the tagged basic device performs CCA2 at the ith backoff stage, after k idle slots since the last transmission, where $i \in [0, m]$ and $k \in [1, W_i]$ [12]:

$$\overline{C}_{i,k} = \begin{cases} \overline{K}_{i,0,k-1}, & k \in [1,2], \\ (1-p_{k-1})\overline{K}_{i,0,k-1}, & k \in [3, W_i]. \end{cases} \tag{4}$$

(4) Initial Transmission State. Denoted by $X_{i,k}$, during which the tagged basic device starts to transmit a frame at backoff stage $i \in [0, m]$, after $k \in [2, W_i + 1]$ idle slots since the last transmission [12]:

$$\overline{X}_{i,k} = \begin{cases} \overline{C}_{i,k-1}, & k = 2, \\ (1-p_{k-1})\overline{C}_{i,k-1}, & k \in [3, W_i + 1]. \end{cases} \tag{5}$$

(5) Transmission State. Denoted by T_l, during which the tagged basic device transmits the lth part of a frame, where $l \in [2, L]$. The first part is transmitted in the state $X_{i,k}$ [12]:

$$\overline{T}_l = \begin{cases} \sum_{i=0}^{m} \sum_{k=2}^{W_i+1} \overline{X}_{i,k}, & l = 2, \\ \overline{T}_{l-1}, & l \in [3, L]. \end{cases} \tag{6}$$

The transmission probability τ_k that the tagged basic device transmits after exactly k idle slots since the last transmission for the nonoverlapped part in CAPs can be computed by $\tau_k = 0$, for $k \in [0, 1]$, and for $k \in [2, W_x + 1]$ [12]:

$$\tau_k = \frac{\sum_{i=0}^{m} \overline{X}_{i,k}}{\sum_{i=0}^{m} \left[\overline{X}_{i,k} + \overline{C}_{i,k} + \sum_{j=0}^{W_i-1} \overline{K}_{i,j,k} \right]}. \tag{7}$$

With the above expressions derived for transmission probability τ_k ($\tau_{1,k}$ and $\tau_{2,k}$ for NET1 and NET2, resp.), we can calculate channel busy probability p_k^f ($p_{1,k}^f$ and $p_{2,k}^f$ for NET1 and NET2, resp.) for the nonoverlapped part of CAPs with the tagged basic device in Scenario I (in NET1 and NET2, resp.) with $k \in [0, W_x + 1]$:

$$\begin{aligned} p_{1,k}^f &= 1 - (1 - \tau_{1,k})^{N_1 - 1}, \\ p_{2,k}^f &= 1 - (1 - \tau_{2,k})^{N_2 - 1}. \end{aligned} \tag{8}$$

Since the balance equations for all steady-state probabilities and expressions for $p_{1,k}^f$ and $p_{2,k}^f$, $k \in [0, W_x + 1]$ have been derived, the Markov chain for the tagged basic device can be numerically solved. After the Markov chains are solved, we can calculate the throughput of nonoverlapped part $S_{I,n}^f$ for Scenario I with individualnetwork:

$$S_{\mathrm{I},n}^f = N_n L_d \sum_{i=0}^{m} \sum_{k=1}^{W_i} C_{n,i,k-1} \left(1 - p_{n,k-1}^f\right) \left(1 - p_{n,k}^f\right), \quad n = 1, 2. \tag{9}$$

To analyse energy consumption, we use normalised energy consumption, defined in [17] as the average energy consumed to transmit one slot of payload. The energy consumption of transmitting a frame in a slot (denoted by E_t) and perform a CCA (denoted by E_c) in a slot is set to 0.01 mJ and 0.01135 mJ, respectively [17]. We use the $\eta_{\mathrm{I},n}^f$ to represent the normalised energy consumptions of the nonoverlapped part for Scenario I with NET1 and NET2, respectively:

$$\eta_{\mathrm{I},n}^f = \frac{N_n}{S_{\mathrm{I},n}^f} \sum_{i=0}^{m} \left\{ \sum_{l=2}^{L} E_c B_{n,i,0,l} + \sum_{k=0}^{W_i+1} \left[E_c \left(K_{n,i,0,k} + C_{n,i,k} \right) + L E_t X_{n,i,k} \right] \right\}, \quad n = 1, 2. \tag{10}$$

For the overlapped part of CAPs in Scenario I, we have the transmission probabilities $\tau_{1,k} = \tau_{2,k}$, and we use $p_{n,k}^o$ to denote the new channel busy probabilities:

$$\begin{aligned} p_{1,k}^o &= 1 - (1 - \tau_{1,k})^{N_1 + N_2 - 1}, \\ p_{2,k}^o &= 1 - (1 - \tau_{2,k})^{N_1 + N_2 - 1}. \end{aligned} \tag{11}$$

The Markov chain for the tagged basic device can be numerically solved again with the new channel busy probabilities. The throughput S_{I}^o of the overlapped part for overall system in Scenario I is obtained as follows:

$$S_{\mathrm{I}}^o = (N_1 + N_2) L_d \sum_{i=0}^{m} \sum_{k=1}^{W_i} C_{1,i,k-1} \left(1 - p_{1,k-1}^o\right) \left(1 - p_{1,k}^o\right). \tag{12}$$

For NET1 and NET2, the throughputs of overlapped part S_n^o with Scenario I are obtained, respectively:

$$S_{\mathrm{I},n}^o = \frac{S_{\mathrm{I}}^o N_n}{(N_1 + N_2)}, \quad n = 1, 2. \tag{13}$$

The normalised energy consumptions of overlapped part for Scenario I are defined as $\eta_{\mathrm{I},n}^o$ with NET1 and NET2, respectively:

$$\eta_{\mathrm{I},n}^o = \frac{N_n}{S_{\mathrm{I},n}^o} \sum_{i=0}^{m} \left\{ \sum_{l=2}^{L} E_c B_{1,i,0,l} + \sum_{k=0}^{W_i+1} \left[E_c (K_{1,i,0,k} + C_{1,i,k}) + L E_t X_{1,i,k} \right] \right\}, \quad n = 1, 2. \tag{14}$$

Now, we can combine the nonoverlapped and overlapped part of CAPs together with different overlap ratio g. The various sleep time in BIs with different SOs is also considered. For Scenario I, we have throughputs $S_{\mathrm{I},n}$ of NET1 and NET2 are calculated by

$$S_{\mathrm{I},n} = 2^{\mathrm{SO}_n - \mathrm{BO}_n} \left[(1 - g) S_{\mathrm{I},n}^f + g S_{\mathrm{I},n}^o \right], \quad n = 1, 2. \tag{15}$$

The overall network throughput S_{I} is calculated by

$$S_{\mathrm{I}} = S_{\mathrm{I},1} + S_{\mathrm{I},2}. \tag{16}$$

The normalised energy consumption $\eta_{\mathrm{I},n}$ of Scenario I for NET1 and NET2 is, respectively

$$\eta_{\mathrm{I},n} = 2^{\mathrm{SO}_n - \mathrm{BO}_n} \frac{(1 - g) S_{\mathrm{I},n}^f \eta_{\mathrm{I},n}^f + g S_{\mathrm{I},n}^o \eta_{\mathrm{I},n}^o}{S_{\mathrm{I},n}}, \quad n = 1, 2. \tag{17}$$

4.2. Analytic Model of Scenario II. So far we have presented the performance analytic mode for Scenarios I with different sleep time and different overlap ratios. In this subsection we will give the analytic mode for Scenario II. Firstly, we assume that the two networks are fully overlapped in the CAPs ($g = 1$), and we focus on the channel access periods only. The performance with different overlap ratios can be obtained after we get the fully overlapped performance. As we discussed previously in Scenario I the channel access operation is not affected by channel activities at other networks. But for Scenario II correct reception of frame transmissions in one network can be affected by the frame transmissions in the other network. If a frame from the tagged basic device transmitted to coordinator in one network does not collide with frames from the other devices in the same network, it is still subject to collide with frames from the other network. An illustration of the uncoordinated operations for Scenario II, is shown in Figure 5. We could reuse the Markov states from [12] and calculate the new channel busy probability $p_{1,k}$ and $p_{2,k}$ for NET1 and NET2 in Scenario II, respectively. The problem that remains to be solved is on the calculation of successful frame reception probability, which depends on the probability of transmissions from both networks.

The performance of NET1 under the impact of uncoordinated operation from NET2 is considered firstly. The impact of NET1 transmissions to NET2 performance can be analysed similarly. With the Markov chain states we can compute the transmission probability $\tau_{2,k}$ of NET2 as done for nonoverlapped part in Scenario I by (7). Now the probability of exact k idle slots before one transmission in the active portion of NET2 can be derived, which is expressed by $p_{2,\mathrm{idle},k} = 0$ (identifier 2 means NET2) for $k \in [0, 1]$ and for $k \in [2, W_x + 1]$:

$$p_{2,\mathrm{idle},k} = \begin{cases} 1 - (1 - \tau_{2,k})^{N_2}, & k = 2, \\ \left(1 - (1 - \tau_{2,k})^{N_2}\right) \prod_{z=2}^{k-1} (1 - \tau_{2,z})^{N_2}, & k \in [3, W_x + 1]. \end{cases} \tag{18}$$

For each transmission from NET2 following k idle slots there is a probability $p_{2,\mathrm{suc},k}$ that an independent transmission from NET1 will not collide with the transmission from NET2. It is noted that the probability $p_{2,\mathrm{suc},k}$ is larger than zero only if idle slots k from NET2 is larger than or equal to the transmission data length L_1 in NET1. An illustration of the collision of frames from NET1 with frames from NET2 is presented in Figure 6.

We can calculate $p_{2,\mathrm{suc},k}$ for $k \in [2, W_x + 1]$ by

$$p_{2,\mathrm{suc},k} = \begin{cases} 0, & k < L_1, \\ \dfrac{k - L_1 + 1}{k}, & k \geq L_1. \end{cases} \tag{19}$$

The average probability $p_{2,\mathrm{suc,avg}}$ that a transmission from NET1 does not collide with transmissions from NET2 can be calculated by

$$p_{2,\mathrm{suc,avg}} = \frac{\sum_{k=2}^{W_x+1} k \cdot p_{2,\mathrm{idle},k} \cdot p_{2,\mathrm{suc},k}}{\sum_{k=2}^{W_x+1} (k + L_2) \cdot p_{2,\mathrm{idle},k}}, \tag{20}$$

where L_2 is the transmission data length in NET2.

For Scenario II, the throughput of nonoverlapped part of each network can be calculated by (9) as done in Scenario I, for there is no interference from each other. Then we can calculate the throughput of overlapped part $S_{\mathrm{II},1}^o$ for NET1 in this scenario:

$$S_{\mathrm{II},1}^o = p_{2,\mathrm{suc,avg}} S_{\mathrm{I},1}^f. \tag{21}$$

Similarly we can use the same way to calculate the throughput of overlapped part S_2^o for NET2:

$$S_{\mathrm{II},2}^o = p_{1,\mathrm{suc,avg}} S_{\mathrm{I},2}^f. \tag{22}$$

After the throughputs of nonoverlapped and overlapped part have been derived, we can calculate the throughputs $S_{\mathrm{II},n}$ for NET1 and NET2. For the different overlap ratio g and sleep time, the throughputs for NET1 and NET2 $S_{\mathrm{II},n}$ in Scenario II can be calculated by

$$S_{\mathrm{II},n} = 2^{\mathrm{SO}_n - \mathrm{BO}_n} \left[(1 - g) S_{\mathrm{I},n}^f + g S_{\mathrm{II},n}^o \right], \quad n = 1, 2. \tag{23}$$

The overall system throughput for Scenario II is calculated by $S_{\mathrm{II}} = S_{\mathrm{II},1} + S_{\mathrm{II},2}$.

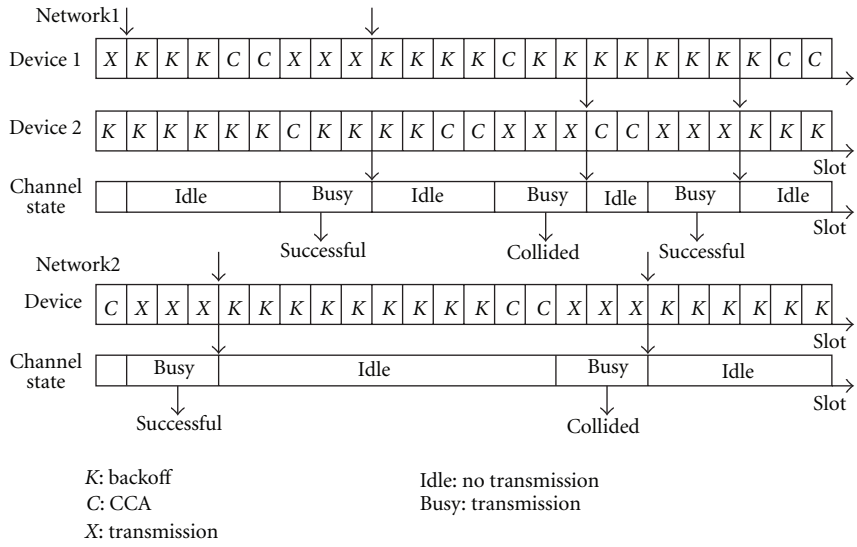

Figure 5: Example of transmission collisions for two uncoordinated 802.15.4 networks for Scenario II.

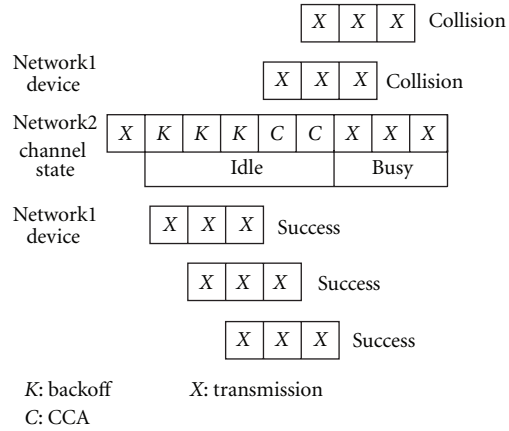

Figure 6: Illustration of transmissions from NET1 with/without collisions with frames from NET2 for Scenario II.

Because of the only impact on the transmissions in each network for Scenario II is the outcomes of frame reception. The normalised energy consumptions $\eta_{\mathrm{II},n}$ for NET1 and NET2 in Scenario II can be calculated by using $\eta^{f}_{\mathrm{I},n}$ (10) in Scenario I with the new throughputs $S_{\mathrm{II},n}$ in Scenario II:

$$\eta_{\mathrm{II},n} = 2^{\mathrm{SO}_n - \mathrm{BO}_n} \frac{\eta^{f}_{\mathrm{I},n} S^{f}_{\mathrm{I},n}}{S_{\mathrm{II},n}}, \quad n = 1, 2. \tag{24}$$

5. Numerical Results and Performance Analysis

We consider an IEEE PHY at frequency band 2400–2483.5 MHz with O-QPSK modulation and data rate of 250 kbps. A discrete event simulator is used to investigate the performance of uncoordinated problem and verify the proposed analytic model. The symbol rate is 62500 symbols per second for the PHY and at most 3000 slots of data could be transmitted in one second. We set BO for each network is fixed 6, which means each superframe length BI is fixed 3072 slots for both NET1 and NET2. Then the CAP of each superframe is only decide by SOs. For example, if SO sets to 5, which means half of the superframe 1536 slots are active portion and the rest is inactive portion. We can vary different SOs for various sleep slots for both two networks to investigate the impact of sleep mode. Typical results are presented with default MAC parameters for NET1: $W_0 = 2^3$, $W_x = 2^5$, and $m = 4$. The MAC parameter in NET2 are varied to investigate the impact of uncoordinated operations from NET2. The overhead of the header L_h in a data frame is 1.5 slots and the data length with MAC and PHY layer herder is $L = L_d + L_h$. We assume that both networks transmit frames with the same data length L. Each simulation results presented in the figures was obtained from the average of 20 simulations. In each simulation 10^5 data frames are transmitted.

Figures 7(a)–7(d) give the normalised throughput and normalised energy consumption of Scenario I. Figures 8(a)–8(d) show the normalised throughput and normalised energy consumption of Scenario II.

5.1. Analysis of Scenario I. Figure 7(a) shows the throughput S of overall system and throughput S_1 of NET1 for Scenario I. Only 5 M2M devices are in NET2 and the MAC parameters of NET2 are as same as those in NET1. For $L = 3$, we have $L_d = 1.5$ and the data length in one frame is 15 bytes. Similarly for $L = 6$, the data length is 55 bytes. Half of the slots in BI are in inactive portion with SO = 5 and CAPs of NET1 and NET2 are fully overlapped with $g = 1$. Consider the case of 20 M2M devices working in NET1. The throughput of NET1 is 0.03 for $L = 3$, which means that at most 30 data messages could be successfully delivered in one second in total NET1. Each M2M device in NET1 could deliver at most 1.5 data messages in one second with message size $L = 3$. This performance may be reasonably acceptable for M2M applications, for most of

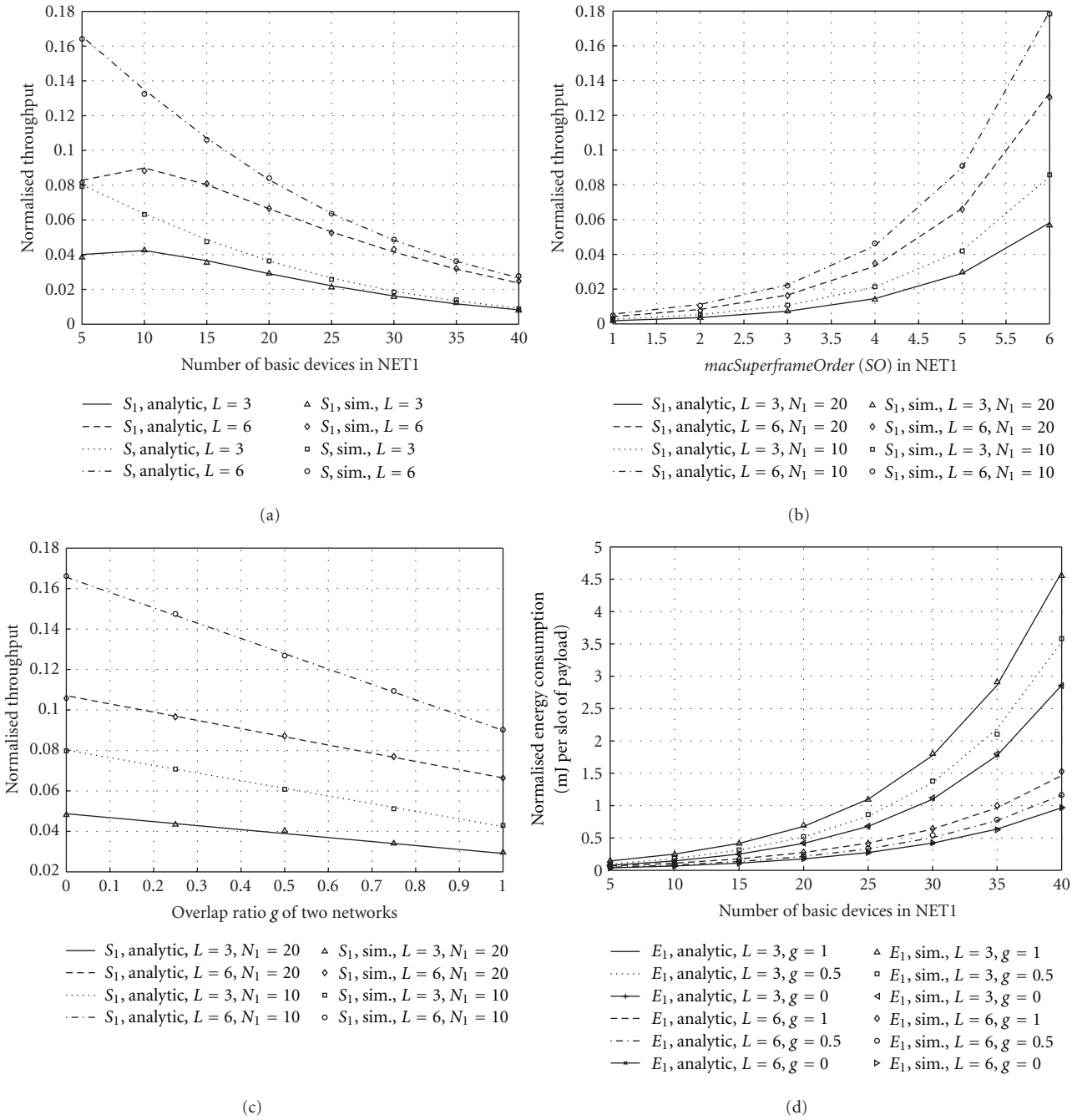

FIGURE 7: Normalised throughput S of overall system, S_1 of NET1 and energy consumption E_1 of NET1 for Scenario I. The number of basic devices in NET2 is fixed 5. (a) $L = 3$, $L = 6$ slots, SO = 5, and $g = 1$ for each network. (b) $L = 3$, $L = 6$ slots, and $g = 1$ for each network. The number of basic devices in NET1 is $N_1 = 20$ and $N_1 = 10$, respectively. (c) $L = 3$, $L = 6$ slots, and SO = 5 for each network. The number of basic devices in NET1 is $N_1 = 20$ and $N_1 = 10$, respectively. (d) $L = 3$, $L = 6$ slots, and $g = 1$; $g = 0.5$, $g = 0$, and SO = 5 for each network.

them do not need high data rate such as smart metering and environment monitoring. However, the throughput of NET1 decreases further when there are more M2M devices and the normal applications may not be effectively supported by the uncoordinated operation in Scenario I.

Figure 7(b) presents the throughput S_1 of NET1 with different SOs in Scenario I. Consider the case of 20 and 10 M2M devices in NET1 as examples. When the SO increased by one (not over maximum BO), the throughput is doubled with the condition overlap ratio $g = 1$. With the assumption of Scenario I, reducing the sleep time or using the nonsleep mode will dramatically increase the throughput S_1 of NET1, which will make it more suitable for most M2M application. For example, if we set SO = 6 for Scenario I, which

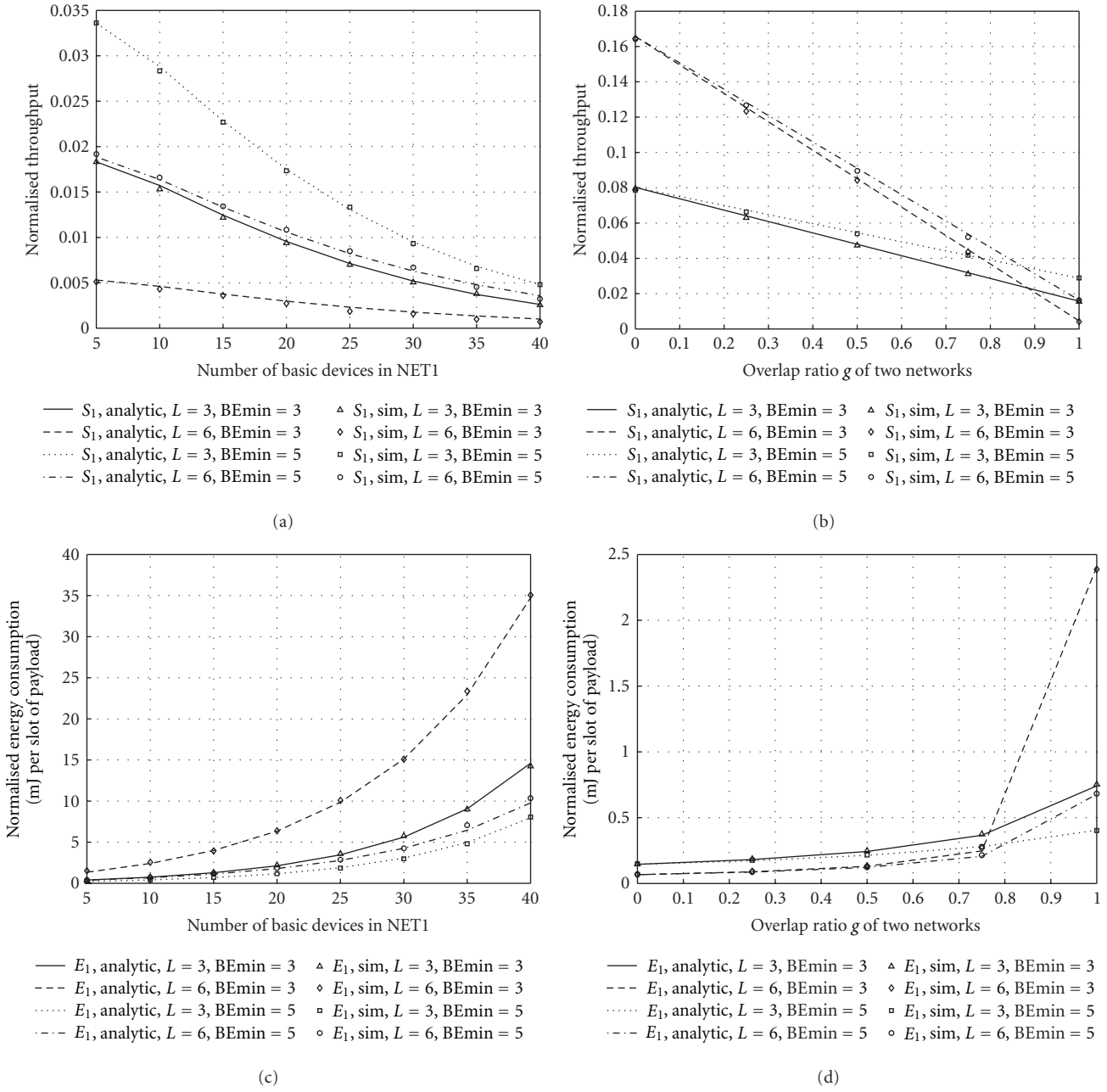

Figure 8: Normalised throughput S_1 of NET1 and energy consumption E_1 of NET1 for Scenario II. The number of basic devices in NET2 is fixed 5 and the BEmin of NET2 is set to 3 and 5 with initial backoff windows are $W_0 = 2^3$ and $W_0 = 2^5$. (a) $L = 3$, $L = 6$ slots and SO = 5, $g = 1$ for each network. (b) $L = 3$, $L = 6$ slots and SO = 5 for each network. The number of basic devices in NET1 is $N_1 = 10$. (c) $L = 3$, $L = 6$ slots, $g = 1$, and SO = 5 for each network. (d) $L = 3$, $L = 6$ slots, and SO = 5 for each network. The number of basic devices in NET1 is $N_1 = 10$.

means these two networks are working in nonsleep mode, the throughput S_1 of NET1 will be doubled than what Figure 7(a) shows, for the active slots in superframe BIs are doubled.

Figure 7(c) shows the relationship between throughput S_1 of NET1 and overlap ratio g in Scenario I. We take $N_1 = 20$ and $N_1 = 10$ as examples. When $g = 0$, which means there is no interference between two networks and when $g = 1$, which means the CAPs are fully overlapped. With the increasing of g from 0 to 1, the throughput S_1 of NET1 linearly drops. Consider the case of 10 M2M devices in NET1. The throughput S_1 of NET1 is 0.08 for $L = 3$ and $g = 0$ which means at most 80 data messages could be successfully transmitted in total in NET1. When the overlap ratio increases to $g = 0.5$ and $g = 1$, the successfully transmitted data messages drop to about 60 and 40, respectively.

Figure 7(d) represents the energy consumption E_1 of NET1 for Scenario I. We consider the cases of $N_1 = 20$ with $L = 3$ for three conditions $g = 1, g = 0.5$, and $g = 0$.

When $g = 1$, the E_1 is at most 0.7 mJ, which is the highest one compared to nearly 0.5 mJ for $g = 0.5$ and about 0.4 mJ for $g = 0$. For Scenario I, it is observed that increasing the active slots in superframe and reducing the overlap ratio can both obtain higher throughputs. Reducing sleep time will not affect the normalised energy consumption, but will increase the total energy consumption, for more slots will be active in superframes. Taking 20 M2M devices with $L = 3$ in NET1 as an example from Figure 7(d), the throughput will be doubled from 0.03 to 0.06 when SO increases from 5 to 6, which means 30 data messages will be increased to 60 data messages that could be successfully delivered in one second in total NET1 with message size $L = 3$. The normalised energy consumption is at most 0.7 mJ for this example with $g = 1$, and it will not change for different SOs. With the SO = 5 at most 10.5 mJ per second energy will be consumed in total of NET1, and when SO = 6 at most 21 mJ per second energy will be consumed in total of NET1. Compared to increase SOs, reducing the overlap ratio can also reduce the energy consumption to get higher throughputs.

5.2. Analysis of Scenario II. Figure 8(a) shows that the throughput S_1 of NET1 in Scenario II with 5 basic devices in NET2. Two sets of initial backoff window (BEmin = 3 and BEmin = 5) are used to study the impact of the slotted CSMA-CA parameters set for NET2 on the NET1 performance. It shows that for BEmin = 3 and $L = 3$, the throughput S_1 of NET1 drops below 0.04 even with only 5 devices in NET1. Results for throughput S of overall system have been obtained but not resented here due to concern on the readability of the figure. With larger frame length $L = 6$, the NET1 throughput S_1 drops further. It is also observed that the analytic results match very well with the simulation results, which demonstrates the high accuracy of the proposed analytic mode. Consider the case of 10 M2M devices in the NET1. The throughput of NET1 is 0.015 for $L = 3$ and 0.005 for $L = 6$, respectively. It means each M2M device in NET1 could successfully deliver at most 1.2 data messages in one second for $L = 3$ and 0.25 data messages for $L = 6$, respectively. When there are more M2M devices the NET1, the throughput of NET1 drops further and the normal M2M applications could not be effectively supported by the 802.15.4 networks. The above analysis shows that for Scenario II, uncoordinated operation of 802.15.4 networks can significantly affect the effectiveness of the networks on supporting M2M applications.

It is observed that with increased random backoff window in NET2, the throughput S_1 of NET1 for Scenario II is largely improved. This can be explained by the fact that with large random backoff window for devices in NET2, there will be smaller collision probabilities between frames from NET1 and NET2. Increasing random backoff window may be an effective measure to improve the system performance in case of multiple uncoordinated 802.15.4 networks and hidden terminals. But it is noted that such improvement may be achieved at cost of increased message delivery delay due to the larger backoff windows. Compared to Scenario I, the throughput S_1 of NET1 is limited even with increased random backoff window in NET2.

Figure 8(b) gives the throughput S_1 of NET1 with different overlap ratio g for Scenario II. The number of basic devices in NET2 is still 5 and in NET1 is 10 as an example. With the increasing of g from 0 to 1, the throughput S_1 of NET1 linearly drops dramatically. When $g = 0.5$, the throughputs S_1 of NET1 for $L = 3$ are about 0.045 and 0.055 with BEmin = 3 and BEmin = 5, respectively. It means each M2M device could successfully transmit 4.5 data messages and 5.5 data message in one second, respectively. When g increases to 1, they drop to 1.5 data messages and 3 data messages in one second, respectively. The throughputs S_1 of NET1 with BEmin = 3 drop quickly than with BEmin = 5 for both $L = 3$ and $L = 6$. With larger frame length ($L = 6$), the NET1 throughput S_1 drops further with increasing g and becomes lower than $L = 3$ when g is near 1.

Figures 8(c) and 8(d) represent the energy consumption E_1 of NET1 for Scenario II. It is observed that the uncoordinated operation of 802.15.4 networks could lead to significant increase of the energy consumption. With increasing number of M2M devices in NET1, the energy consumption E_1 of NET1 will increase dramatically and hardly support M2M application. For larger backoff window in NET2 (BEmin = 5), the energy consumption E_1 of NET1 largely drops, for more data messages can be successfully transmitted without collision. It is still higher compared to Scenario I. The overlap ratio can affect the energy consumption significantly, with lower overlap ratio g, the energy consumption can be largely improved. Compared to the measure of increasing random backoff window in NET2, the adaptive sleep mode which can decrease the overlap ratio g may be a more effective way to improve the system performance of both throughput and energy consumption.

6. Conclusion

Wireless M2M networks could play a critical role in the M2M technology. In this paper, we investigated the effectiveness of IEEE 802.15.4 networks in support of M2M communications. Two representative scenarios of closely deployed and uncoordinated IEEE 802.15.4 networks are studied. An analytic mode was proposed to understand the impact of uncoordinated operations and sleep mode on the overall system performance. Simulations demonstrate the high accuracy of the proposed analytical model. It was observed that the uncoordinated operations of 802.15.4 networks have significant impact on the M2M application performances. Reducing sleep time and overlap ratio can improve the overall networks performances. But by reducing sleep time approach the energy consumption may be increased due to longer active periods. On the other hand reducing sleeping overlap ratio g in the channel access periods of networks can largely improve the throughput and decrease the energy consumption.

Acknowledgments

The work was supported by the UK Engineering and Physical Sciences Research Council (EPSRC) with Grant reference no. EP/1010157/1 and the National Natural Science Foundation of China (NSFC) under the Grant no. 61103177.

References

[1] R. Q. Hu, Y. Qian, H. H. Chen, and A. Jamalipour, "Recent progress in machine-to-machine communications," *IEEE Communications Magazine*, vol. 49, no. 4, pp. 24–26, 2011.

[2] R. Lu, X. Li, X. Liang, X. Shen, and X. Lin, "GRS: the green, reliability, and security of emerging machine to machine communications," *IEEE Communications Magazine*, vol. 49, no. 4, pp. 28–35, 2011.

[3] Z. M. Fadlullah, M. M. Fouda, N. Kato, A. Takeuchi, N. Iwasaki, and Y. Nozaki, "Toward intelligent machine-to-machine communications in smart grid," *IEEE Communications Magazine*, vol. 49, no. 4, pp. 60–65, 2011.

[4] S. Y. Lien and K. C. Chen, "Massive access management for QoS guarantees in 3GPP machine-to-machine communications," *IEEE Communications Letters*, vol. 15, no. 3, pp. 311–313, 2011.

[5] "IEEE standard for information technology- local and metropolitan area networks- specific requirements- part 15. 4: wireless medium access control (mac) and physical layer (phy) specifications for low rate wireless personal area networks (wpans)," IEEE Standards 802. 15. 4-2006 (Revision of IEEE Std 802. 15. 4-2003), vol. 7, pp. 1 –320, 2006.

[6] J. Zheng and M. Lee, "A comprehensive performance study of IEEE 802. 15. 4," *Sensor Network Operations*, pp. 218–237, 2004.

[7] G. Anastasi, M. Conti, and M. Di Francesco, "A comprehensive analysis of the MAC unreliability problem in IEEE 802.15.4 wireless sensor networks," *IEEE Transactions on Industrial Informatics*, vol. 7, no. 1, pp. 52–65, 2011.

[8] K. Yedavalli and B. Krishnamachari, "Enhancement of the IEEE 802.15.4 MAC protocol for scalable data collection in dense sensor networks," in *Proceedings of the Symposium on Modeling and Optimization in Mobile, Ad Hoc, and Wireless Networks (Wiopt'08)*, pp. 152–161, April 2008.

[9] J. Mišić, S. Shafi, and V. B. Mišić, "Performance of a beacon enabled IEEE 802.15.4 cluster with downlink and uplink traffic," *IEEE Transactions on Parallel and Distributed Systems*, vol. 17, no. 4, pp. 361–376, 2006.

[10] I. Das and S. Roy, "Analysis of the contention access period of ieee 802. 15. 4 mac," Tech. Rep. UWEETR-2006-0003, Department of Electrical Engineering, University of Washington, 2006.

[11] Z. Tao, S. Panwar, D. Gu, and J. Zhang, "Performance analysis and a proposed improvement for the IEEE 802.15.4 contention access period," in *Proceedings of the IEEE Wireless Communications and Networking Conference (WCNC'06)*, pp. 1811–1818, April 2006.

[12] J. He, Z. Tang, H. H. Chen, and S. Wang, "An accurate Markov model for slotted CSMA/CA algorithm in IEEE 802.15.4 networks," *IEEE Communications Letters*, vol. 12, no. 6, pp. 420–422, 2008.

[13] S. Pollin, M. Ergen, S. C. Ergen et al., "Performance analysis of slotted carrier sense IEEE 802.15.4 medium access layer," *IEEE Transactions on Wireless Communications*, vol. 7, no. 9, pp. 3359–3371, 2008.

[14] C. K. Singh, A. Kumar, and P. M. Ameer, "Performance evaluation of an IEEE 802.15.4 sensor network with a star topology," *Wireless Networks*, vol. 14, no. 4, pp. 543–568, 2008.

[15] P. Park, P. Di Marco, P. Soldati, C. Fischione, and K. H. Johansson, "A generalized Markov chain model for effective analysis of slotted IEEE 802.15.4," in *Proceedings of the IEEE 6th International Conference on Mobile Adhoc and Sensor Systems (MASS '09)*, pp. 130–139, October 2009.

[16] J. He, Z. Tang, H. H. Chen, and Q. Zhang, "An accurate and scalable analytical model for IEEE 802.15.4 slotted CSMA/CA networks," *IEEE Transactions on Wireless Communications*, vol. 8, no. 1, pp. 440–448, 2009.

[17] T. R. Park, T. H. Kim, J. Y. Choi, S. Choi, and W. H. Kwon, "Throughput and energy consumption analysis of IEEE 802.15.4 slotted CSMA/CA," *Electronics Letters*, vol. 41, no. 18, pp. 1017–1019, 2005.